Induced circularly polarized luminescence arising from anion or protein binding to racemic emissive lanthanide complexes

2014 Methods Appl. Fluoresc. 2 024007

(http://iopscience.iop.org/2050-6120/2/2/024007)

OPEN ACCESS
IOP Publishing
Made open access 12 December 2014
Methods and Applications in Fluorescence
Methods Appl. Fluoresc. **2** (2014) 024007 (7pp)
doi:10.1088/2050-6120/2/2/024007

Induced circularly polarized luminescence arising from anion or protein binding to racemic emissive lanthanide complexes

Rachel Carr, Robert Puckrin, Brian K McMahon, Robert Pal, David Parker and Lars-Olof Pålsson

Department of Chemistry, Durham University, South Road, Durham DH1 3LE, UK

E-mail: david.parker@durham.ac.uk and lars-olof.palsson@durham.ac.uk

Received 27 October 2013, in final form 13 December 2013
Accepted for publication 18 December 2013
Published 9 April 2014

Abstract

A circularly polarized luminescence (CPL) spectrometer has been built and used to study the binding interaction of lactate and four different proteins with racemic Eu^{III} and Tb^{III} complexes in aqueous solution. Lactate binding gives rise to strong induced CPL spectra, and the observed emission dissymmetry factors vary linearly with enantiomeric composition. Particularly strong induced Tb^{III} CPL also characterizes the binding interaction of alpha-1-acid glycoprotein with a dissociation constant, K_d, of 2.5 μM.

Keywords: circular polarisation, lanthanide complexes, chiral interactions, optical spectroscopy, biological systems

(Some figures may appear in colour only in the online journal)

1. Introduction

The use of circularly polarized light in optical spectroscopy is most commonly found in circular dichroism spectroscopy. Using this technique, the character of the electronic ground state can be elucidated, providing an understanding of the molecular conformations of chiral systems. An example where this is applied successfully is in the assessment of the structural properties of biological macromolecules, such as proteins. A related, but less widely used, technique involves monitoring the circularly polarized luminescence (CPL) of chiral emissive chromophores [1, 2]. CPL spectroscopy is inherently much more sensitive than CD. This is due to the fact that the excited state behaviour can be modulated by a number of factors, such as polarity and medium effects or static or dynamic quenching. The latter may occur on timescales similar to the excited state lifetime. Such behaviour is readily exploited in sensing applications of dielectric media with fluorescence as the key signalling tool. Perhaps the most striking difference, in this context, is that with CD the background from the medium or matrix (of, for instance, biological systems) would contribute extensively to the optical signature, dwarfing the CD signal from the chiral probe. With CPL it is possible to achieve selective excitation and detection of the sensing emissive complex, which ensures a unique signal, free from background interference. This is of obvious utility when attempting to detect chiral species *in vivo*.

A promising class of chiral emissive probes is based on functionalised lanthanide (Ln^{III}) complexes, particularly strongly emissive europium (Eu^{III}) and terbium (Tb^{III}) systems [3–5]. Versatile Ln^{III}-based probes are emerging for imaging and sensing studies of bio-active systems and are already being used in a wide variety of biological assays [6–10]. The photoluminescence (PL) of Eu^{III} and Tb^{III} complexes is characterised by sharp emission lines from the 4f electron manifold which are shielded from strong matrix interactions. Due to the Laporte forbidden nature of f–f electronic transitions, the PL lifetime is relatively long ($\sim 10^{-3}$ s). Energy levels of the Ln^{III} ground and excited states are generally considered by invoking a Russell–Saunders coupling scheme. The splitting of the Ln^{III} ion energy levels with the largest impact is due to electrostatic repulsion ($\sim 10^4$ cm^{-1}). A second level of splitting is associated with spin–orbit coupling ($\sim 10^3$ cm^{-1}). Furthermore, crystal field effects associated with the local lattice or ligand (i.e. symmetry, ligand constitution and donor polarisability) can also cause hyperfine

splitting (~100–700 cm^{-1}). For Eu^{III} this leads to the following principal electronic emission transitions: $^5D_0 \rightarrow {}^7F_J$, while for Tb^{III} the energy gap is slightly larger and the possible emission transitions are: $^5D_4 \rightarrow {}^7F_J$. Here, J denotes the total angular momentum and is a key parameter in this context; for transitions with $\Delta J = \pm 1$, we obtain the magnetic dipole (MD) allowed transitions, while for $\Delta J = 2, 4, 6$, we obtain the electric dipole (ED) allowed transitions. A consequence of the presence of the ligand field and the degree of J mixing that may occur is that many of the observed transitions possess a mixture of both MD and ED character—this has a fundamental consequence for the CPL of functionalised Ln^{III} complexes.

According to the Rosenfeld formalism, the microscopic origin of the circular polarisation depends on the rotational strength parameter, R_{ge}, of the electronic transition $|g\rangle \rightarrow |e\rangle$, which is expressed as

$$R_{ge} = \text{imag}(\langle g|\bar{\mu}|e\rangle\langle e|\bar{m}|g\rangle). \quad (1)$$

The key aspect is that R_{ge}, depends on the scalar product of the MD transition moment vector ($\bar{m}$) and an ED transition moment vector ($\bar{\mu}$). As these prerequisites are present in the electronic transitions of Ln^{III} ions, it is possible to observe very strong circular polarisation of the emission.

The degree of polarisation of the macroscopic emission intensity is quantified using the emission dissymmetry factor, g_{em}, which is given by

$$g_{em} = \frac{2(I_L - I_R)}{I_L + I_R} \quad (2)$$

where I_L and I_R denote the left and right hand polarisations respectively. Microscopically, the rotational strength is related to the emission dissymmetry factor as follows:

$$g_{em} = \frac{4R_{ge}}{|\bar{\mu}_{ge}|^2}. \quad (3)$$

As the rotational strength R_{ge} depends on the MD transition, the emission dissymmetry factor is scaled accordingly (equation (4)) [2], as follows:

$$g_{em} = \frac{4|\bar{m}_{ge}|}{|\bar{\mu}_{ge}|}\cos\theta \quad (4)$$

where θ is the mutual orientation angle between ED and MD transition dipole moments. For Ln^{III} complexes, a g_{em} value of 1.4 has been reported [11] (the maximum value is 2, as evident from equation (2)) and typical values are in the range 0.05–0.6. These values should be compared to purely organic chromophores, which display considerably less polarisation of the emission (g_{em} values of 0.001–0.01) and, as non-spherical emitters, require consideration of the anisotropy of the emission.

The emission spectra of certain Ln^{III} complexes exhibit a remarkable sensitivity to their environment, and intermolecular interactions can cause modulations of the PL intensity, lifetime and spectral form. For Eu^{III} complexes this is particularly significant. For example, variation of the axial donor in the complex can have a major impact on the intensity of the $^7F_2 \leftarrow {}^5D_0$ transition [12]. This property has been successfully exploited in signalling reversible anion binding in aqueous media, leading to several examples of anion-sensing [13–16]. Equally, interactions with proteins such as human serum albumin (HSA) and acute phase proteins have been reported [17], facilitated by an electrostatic interaction between the positively charged Ln^{III} complex and the negatively charged side chains of the proteins. In both of the aforementioned examples, the interaction is evident from a modulation of the PL, typically monitored by assessing variations in the emission intensity ratio of two or more bands, or via changes in the emission lifetime. However, this analysis (though successful) is not normally sensitive to stereochemical aspects that arise from chiral interactions.

Following a stereoselective interaction between a chiral (bio) molecular structure and a functionalised Ln^{III} complex, a CPL signal can be either induced or modulated, according to different scenarios [2]. A racemic mixture of Ln^{III} complexes in an achiral environment will not exhibit any CPL, as there is a cancellation of polarisation directions. However, with the addition of a chiral agent, the equilibrium is perturbed and a net CPL signal may be obtained. In a similar manner, excitation of a racemic system with CP light can lead to CPL, where the observed CPL is a function of the product of g_{abs} and g_{em} [1]. Alternatively, the interaction of a chiral Ln^{III} complex with an enantio-enriched molecule can result in a change in the CPL signal. This can be attributed to changes in the coordination structure, i.e. the constitution of the complex, associated with reversible binding of the chiral moiety to the metal centre. Thus, a Δ or Λ (indicating the helicity of the complex [2]) Ln^{III} complex with an inherent CPL will display CPL signal modulation, as changes to the inner coordination structure generally perturb the ligand field considerably. Owing to the relative simplicity of Eu^{III} total emission and CPL spectra, arising from the absence of degeneracy of the $^5D_0$ emissive state, such changes are often best observed with Eu^{III} examples, in the first instance.

There are two aspects to this present contribution. Firstly, the design and commissioning of a home-built modular CPL spectrometer is described. A key point in this endeavour was to ensure that reliable polarisation parameters of the emission were measured. The validation procedure undertaken is described herein. Secondly, the stereospecific interactions between functionalised Ln^{III} complexes and chiral agents were studied using CPL spectroscopy. These Ln^{III} complexes are distinguished by different modes of operation [2]. As a consequence of the binding interaction a CPL signal was turned on, with specific signatures resulting from the handedness of the chiral agents.

2. Methods and materials

CPL was measured with a home-built (modular) spectrometer (see figure 1 for the experimental layout). The excitation source was a broadband (200–1000 nm) laser-driven light source EQ 99 (Elliot Scientific). The excitation wavelength was selected by feeding the broadband light into an Acton SP-2155 monochromator (Princeton Instruments);

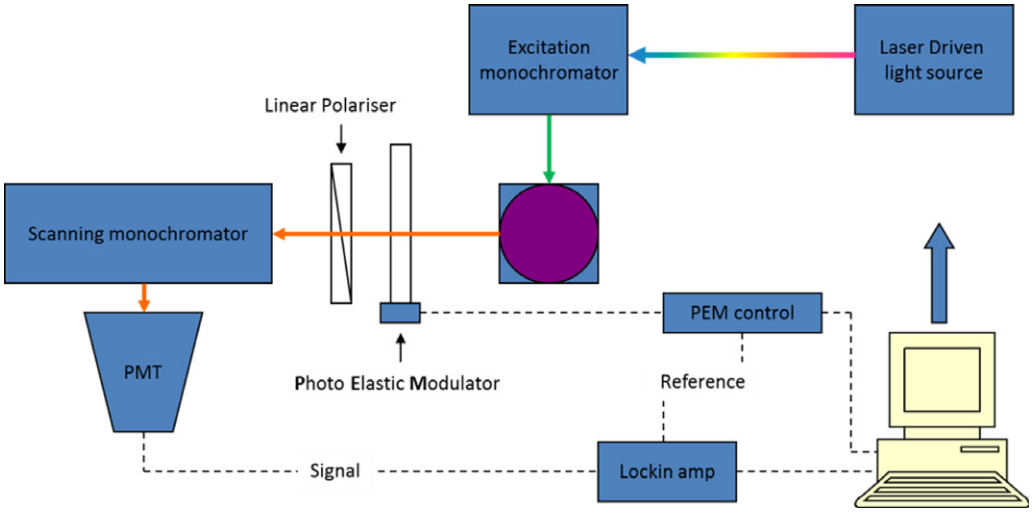

Figure 1. Schematic outline of the modular CPL spectrometer. Coloured lines indicate excitation and emission light pathways; dashed lines electronic signal pathways. See section 2 for details.

the collimated light was focused into the sample cell (1 cm quartz cuvette). Sample PL emission was collected perpendicular to the excitation direction with a lens ($f = 150$ mm). The emission was fed through a photoelastic modulator (PEM) (Hinds Series II/FS42AA) and through a linear sheet polariser (Comar). The light was then focused into a second scanning monochromator (Acton SP-2155) and subsequently on to a photomultiplier tube (PMT) (Hamamatsu H10723 series). The detection of the CPL signal is achieved using the field modulation lock-in technique. The electronic signal from the PMT was therefore fed into a lock-in amplifier (Hinds Instruments Signaloc Model 2100). The reference signal for the lock-in detection was provided by the PEM control unit. The monochromators, PEM control unit and lock-in amplifier were interfaced to a desktop PC and controlled by a Labview code. The lock-in amplifier provided two signals, an AC signal corresponding to $I_{\mathrm{L}} - I_{\mathrm{R}}$ and a DC signal corresponding to $I_{\mathrm{L}} + I_{\mathrm{R}}$ after background subtraction. The emission dissymmetry factor was therefore readily obtained from the experimental data as

$$g_{\mathrm{em}} = \frac{2 \times \mathrm{AC}}{\mathrm{DC}}. \tag{5}$$

Spectral calibration of the scanning monochromator was performed using a Hg–Ar calibration lamp (Ocean Optics). A correction factor for the wavelength dependence of the detection system was constructed using a calibrated lamp (Ocean Optics). The measured raw data were subsequently corrected using this correction factor. The validation of the CPL detection systems was achieved using light emitting diodes (LEDs) at various emission wavelengths. The LED was mounted in the sample holder and the light from the LED was fed through a broadband polarising filter and $\lambda/4$ plate (Ocean Optics) to generate circularly polarized light. An example of this is shown in figure 2. The emission dissymmetry factor for the spectra in figure 2 is $g_{\mathrm{em}} = 1.7$, and similar values were obtained for the other colour LEDs across the visible spectrum. The theoretical maximum for the emission dissymmetry factor

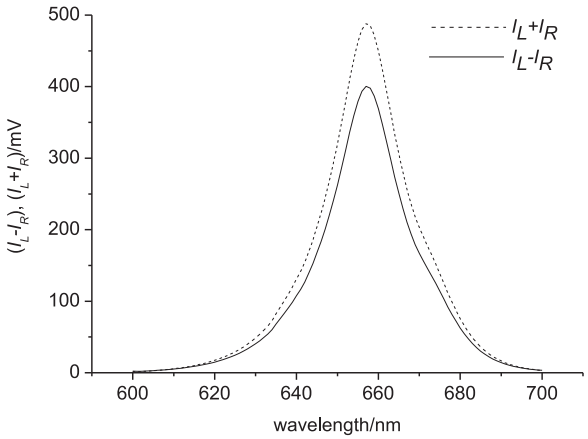

Figure 2. Spectra from a red LED with its emission maximum at 655 nm. Dashed line corresponds to the DC signal; solid line corresponds to the AC signal.

as evident from equation (2) is $g_{\mathrm{em}} = 2$. We remark that the slightly smaller value obtained for the $\lambda/4$ plate is due to fact that this is a broadband filter and thus does not perfectly convert non-polarized light into 100% circularly polarized light. Prior to all measurements, the $\lambda/4$ plate and an LED were used to set the phase of the lock-in amplifier correctly. The emission spectra were recorded with 0.5 nm step size and the slits of the detection monochromator were set to a slit width corresponding to a spectral resolution of 0.25 nm. CPL spectra (as well as DC spectra) were obtained through an averaging procedure of several scans. This was subsequently used to estimate the uncertainty in the g_{em} factor.

Some PL spectra have been measured using a Jobin-Yvon Horiba Fluorolog under similar conditions (excitation wavelength, step size and emission spectral bandwidth).

The synthetic protocol for the design of Ln^{III} complexes $[Ln.L^1(H_2O)]^+$ and $[Eu.L^2(H_2O)]^+$ (scheme 1) are described elsewhere [17, 18] (respectively). Sample materials were dissolved in high-purity water unless otherwise stated. Anions

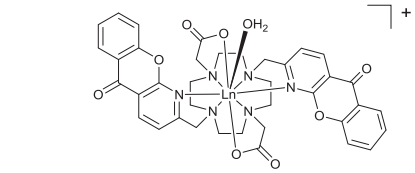

$[Ln.L^1(H_2O)]^+$ Ln = Eu or Tb

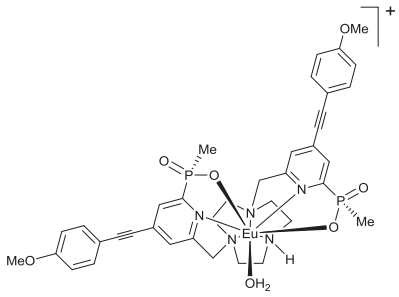

$[Eu.L^2(H_2O)]^+$

Scheme 1. The chemical structures of the two Ln^{III} complexes examined.

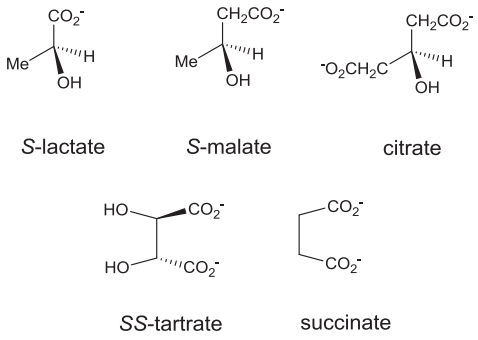

S-lactate *S*-malate citrate

SS-tartrate succinate

Scheme 2. Anions investigated in this study.

(scheme 2) were obtained from Sigma Aldrich and used without further modification/purification.

3. Results and discussion

Two recently described emissive Ln^{III} complexes have been selected for study in this work. In the absence of added chiral material they give no CPL in aqueous solution. The Eu^{III} complex, $[Eu.L^1(H_2O)]^+$, exists in solution as a 50/50 mixture of Δ and Λ enantiomers and is based on an achiral ligand derived from 1,4,7,10-tetraazacyclododecane (cyclen). The complex coordination geometry is a mono-capped square antiprism and interconversion between enantiomers requires dissociation of the Eu-pyridine N bond. In recent work, it has been shown that addition of certain proteins leads to reversible displacement of the water molecule and one of the weakly bound azaxanthone chromophores, followed by chelation of a protein glutamic acid residue [17].

The second example relates to a much brighter Eu^{III} complex, $[Eu.L^2(H_2O)]^+$, which possesses two substituted aryl–alkynyl chromophores, with a brightness of the order of 15 mM^{-1} cm^{-1} in aqueous solution [18]. The ligand is achiral and heptadentate, and, on complexation with Eu^{III}, *SS*-Δ and *RR*-Λ enantiomers form, where *S*/*R* refer to the configuration arising at *P* and Δ/Λ describe the local helicity. The steric demand at the metal centre is greater than in $[Ln.L^1(H_2O)]^+$, and in preliminary work it was shown that both simple carboxylates (e.g. acetate) and α-hydroxy-acids (e.g. lactate) bind to the Eu^{III} in the same manner, via carboxylate binding [18]. Such behaviour contrasts with examples in the extensive series of complexes based on heptadentate cyclen-derived ligands of lower steric demand, where α-hydroxy acids form a five-ring chelate, involving one carboxylate oxygen and the alcohol OH group, as revealed by crystallographic and NMR analyses [19–21]. The binding of a series of α-hydroxy-acids to the Eu^{III} and Tb^{III} complexes of L^1 was examined in water. Incremental addition of solutions of the sodium salts of *S* lactate, malate and tartrate to an aqueous solution of the Ln^{III} complex (295 K 20 μM complex, 0.1 M NaCl) were monitored by following changes in the total emission spectral profile for Tb^{III} and Eu^{III}. In control experiments, the additions of bicarbonate, acetate, succinate and citrate (all achiral) and alanate were also examined.

In each case, it was possible to estimate an apparent binding constant, assuming a 1:1 stoichiometry for the ternary adduct, by fitting the variation of the ratio of the intensity of a separate pair of emission bands with the concentration of added anion (0–80 mM in stepwise titration). Using standard least-squares iterative fitting methods, log K_d values for binding to the Eu complex ranged between 0.65 (alanate) and 1.0 (acetate) to 1.94 for lactate. Values for the other examples were lower (succinate: log $K_d = 1.0$; malate: 1.81; citrate 1.49; tartrate: 0.88; compared to 2.4 for bicarbonate). As the binding constant for tartrate is small and no limiting spectrum was observed, no CPL studies were undertaken. There also appear to be multiple emissive species present for this combination. As two of the acids in scheme 2 (citrate and succinate) are not chiral it is not expected that these would show any CPL; and for that reason they were not studied further with CPL spectroscopy. More importantly, the limiting Eu^{III} emission spectral form for lactate was uniquely simple. It showed three distinct $\Delta J = 1$ components and one $\Delta J = 0$ transition, consistent with the presence of one major species in solution (figure 3).

In all of the other cases, the limiting spectral form (Eu^{III} and Tb^{III}) was almost identical, more than three bands were evident for the Eu^{III} $\Delta J = 1$ manifold, between 588 and 605 nm. Such behaviour suggests a common association mode, which must simply involve carboxylate binding only. In the case of citrate, the observed total emission intensity was particularly weak, suggesting that citrate may displace both of the azaxanthone chromophores, lowering the overall emission quantum yield (ϕ_{em}). Such a situation can arise when the intramolecular energy transfer step is much less efficient, as the distance between the chromophore and the Ln^{III} ion increases.

CPL studies were conducted using the precursor Tb^{III} complex, which has a higher quantum yield ($[Tb.L^1(H_2O)]^+$: $\phi_{em} = 37\%$ compatred to $\phi_{em} = 18\%$ for $[Eu.L^1(H_2O)]^+$ both

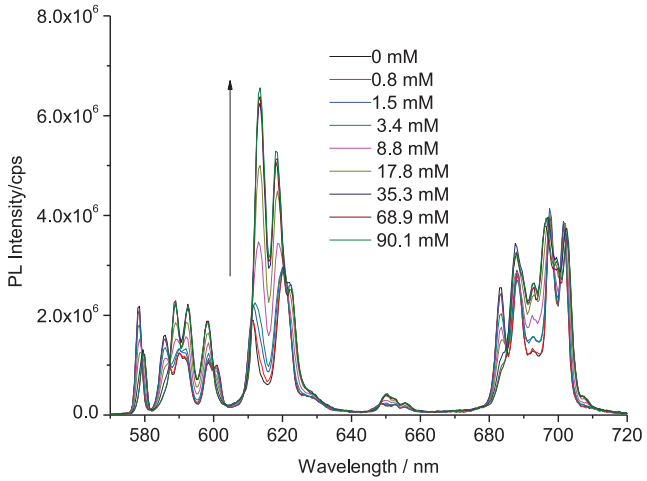

Figure 3. Total PL spectra for [Eu.L^1] following incremental addition of *S*-lactate. The arrow indicates the direction of increasing anion concentration.

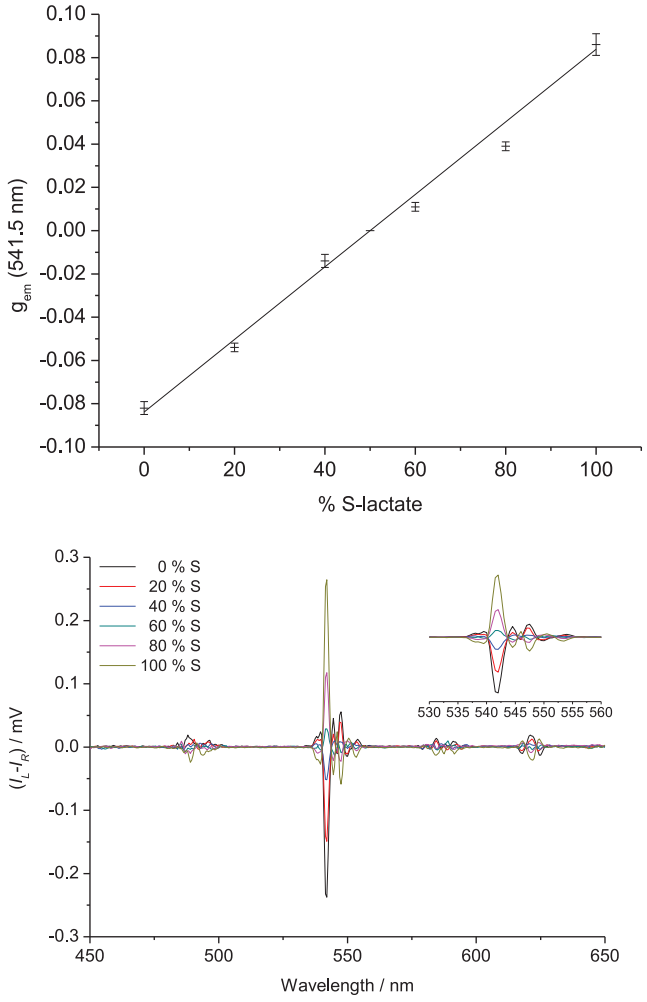

Figure 4. Top: changes in the CPL spectra of [Tb.L^2] as a function of the enantiomeric purity of *S*-lactate. Inset is a magnification of the $\Delta J = -1$ region. Bottom: variation of g_{em} (541.5 nm) with % *S*-lactate, error bars indicate the standard error ($R^2 = 0.97$ for linear fit).

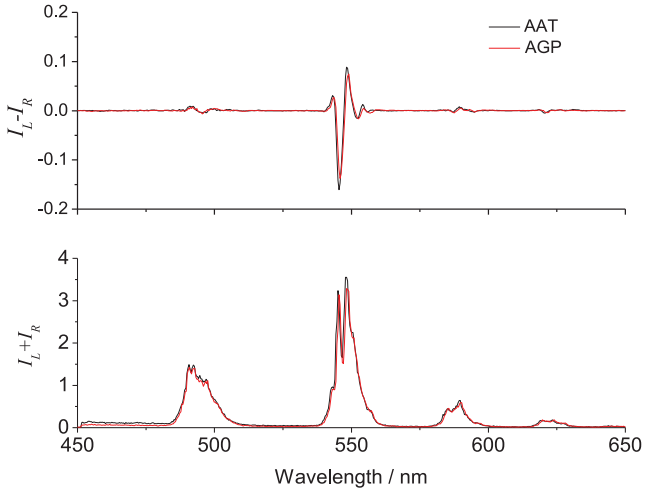

Figure 5. Top: CPL spectra for [Tb.L^1] following addition of either α_1-AAT (black) or α_1-AGP (red). Bottom: total PL spectrum in the same experiment.

in H_2O, 295 K), therefore giving rise to CPL spectra with better signal to noise. The CPL spectrum for [Tb.L^1(H_2O)]$^+$ following addition of *S*-malate was indistinct, presumably due to ill-defined solution speciation. In contrast, separate additions of *R* and *S* lactate exhibited mirror image behaviour. In fact, by adding scalemic samples of lactate of pre-determined enantiomeric composition, it was possible to calibrate the observed g_{em} values (observed at 541.5 nm in the $\Delta J = -1$ Tb^{III} emission manifold, for example) with the enantiomeric purity of the lactate sample, shown in figure 4, and a linear relationship was observed. This implies that, with the modest chemoselectivity observed, such behaviour allows lactate enantiomeric purity to be assessed quickly using this method, for samples of unknown composition. The magnitude of the observed g_{em} values for the Tb^{III} transitions was in the range 0.02–0.08, and the largest values observed were for the transitions within the MD allowed $\Delta J = -1$ manifold.

The behaviour of [Tb.L^1(H_2O)]$^+$ was also examined in the presence of four common proteins. Addition of α_1-alpha acid glycoprotein (AGP) or α_1-antitrypsin (AAT) led to the formation of a protein-bound complex, in which the limiting total emission and CPL spectral forms were identical (figure 5). By measuring the radiative rate constant associated with Tb^{III} emission decay in water and in D_2O [22], it was evident that there was no bound water in each protein adduct; see table 1.

In contrast, Tb^{III} CPL and total emission spectra were weak and ill-defined, following addition of human serum albumin (HSA) or immunoglobulins (γ-IgG). As had been observed with the Eu^{III} analogues [17], the binding of the complex to α_1-AGP was the strongest ($\log K = 5.4$), consistent with a binding model in which the displaced azaxanthone chromophore is bound in the protein drug-binding pocket, and a remote glutarate side chain (e.g. Glu-64) is coordinated to the lanthanide centre. A similar coordination environment must exist with α_1-AAT, and the lower overall free energy of binding probably reflects a less favourable hydrophobic interaction.

In preliminary work, the binding of [Eu.L^2(H_2O)]$^+$ to several anions had shown that α-hydroxy acids did not

Table 1. Binding affinities (295 K, pH 7.4, 0.1 M NaCl) and selected photophysical data defining the interaction of $[Tb.L^1]^+$ with four common proteins.

Protein	log K	$\tau^{Tb}_{H_2O}$ (bound)[a]	g_{em}^{547}	g_{em}^{549}	Speciation
α_1-AGP[b]	5.4	1.79	−0.13	+0.05	One major species
α_1-AAT[b]	4.6	1.83	−0.13	+0.05	One major species
γ-IgG[c]	3.9	—	−0.04	−0.01	Multiple species
HSA[c]	n.d.	—	−0.05	−0.02	Multiple species

[a] With γ-IgG and HSA, multiple exponential decays were observed of similar approximate lifetime, so it was not possible to assign a Tb lifetime value accurately.
[b] Analysis of lifetime data recorded in H_2O and D_2O revealed that in the protein bound adduct there is no coordinated water molecule; e.g. for $[Tb.L^1]$ with α_1-AAT, $k_{H_2O} = 0.55\ ms^{-1}$, and $k_{D_2O} = 0.47\ ms^{-1}$. Hence, using $q = 5(\Delta k - 0.06)$, we find that $q = 0.1$ (± 0.1) [22].
[c] Spectral analysis was not possible here due to significant quenching that reduces observed emission intensity, although it was evident that there were multiple species present in solution, even at high added protein levels.

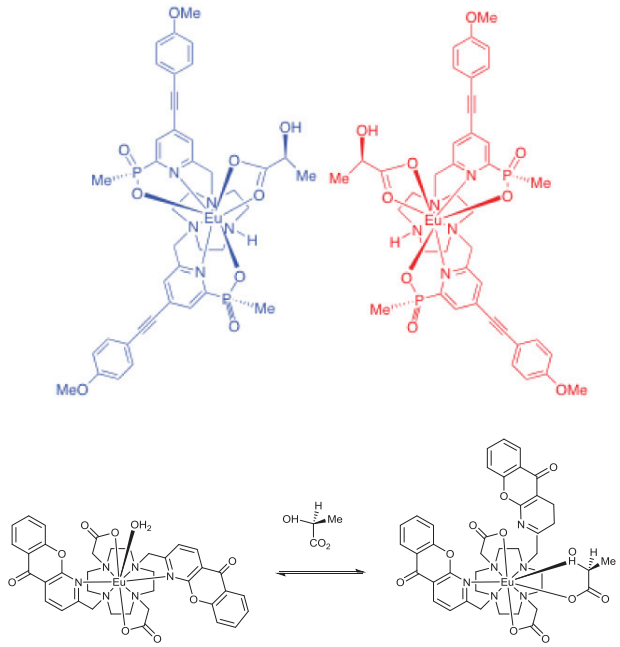

Scheme 3. Top: left *S*-lactate induces formation of the Λ-complex; Bottom: reversible binding of lactate to $[Eu.L^1(H_2O)]^+$, involving water and chromophore displacement.

bind via five-ring chelation [18]. The binding of lactate to $[Eu.L^2(H_2O)]^+$ was monitored by CPL and normal PL spectroscopy, and the change in g_{em} values with lactate enantiomeric composition was again studied. Well-defined changes in Eu^{III} emission spectral form occurred and the induced CPL was equal and opposite for *R* and *S* lactate-bound species (figure 6). The overall affinity constants defining the binding of *R* and *S* lactate were found to be identical (log $K = 2.41$, (± 0.05), 295 K, 0.1 M NaCl).

Analysis of the induced CPL changes was undertaken by examining the change in g_{em} with % ee lactate for a $\Delta J = 2$ transition at 621.5 nm. A linear variation was observed, and this calibration also allows lactate enantiomeric purity in unknown samples to be assessed. Moreover, the relative size, sign and sequence of the observed CPL transitions could

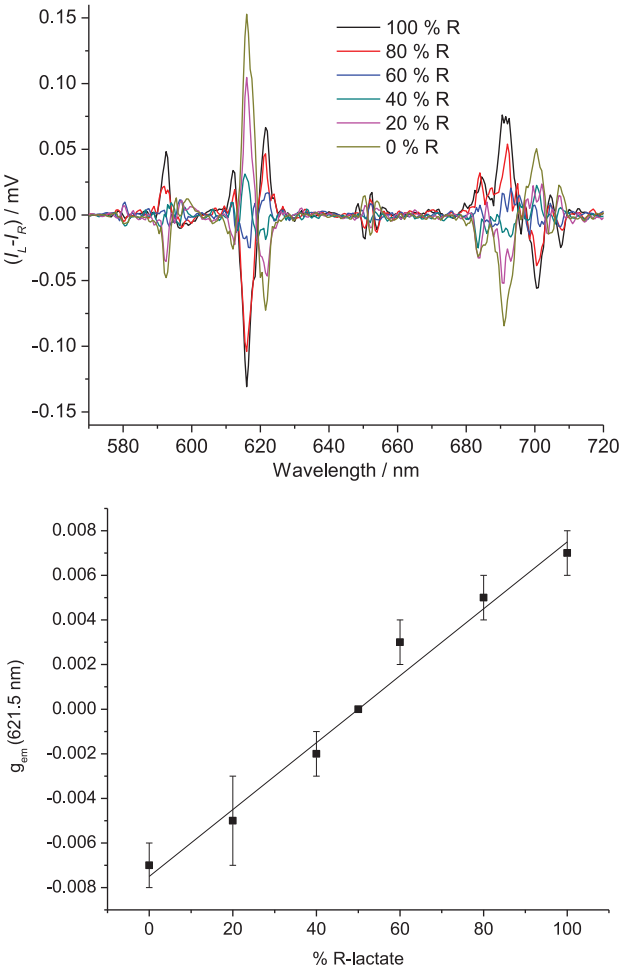

Figure 6. Top: changes in the CPL spectrum of $[Eu.L^2]$ following addition of lactate of varying enantiomeric composition. Bottom: variation of g_{em} (621.5 nm) with % *R*-lactate, error bars indicate the standard error ($R^2 = 0.98$ for linear fit).

be compared to those reported for the Eu^{III} complexes of structurally related, enantiopure tri-substituted ligands (in C_3 symmetry), whose absolute configuration has been assigned by both x-ray crystallography and CD methods [23–25]. Thus, addition of *S*-lactate leads selectively to preferential formation of a Λ-Eu^{III} ternary complex (scheme 3).

The size of the induced CPL is an order of magnitude smaller than that observed for lactate binding to $[Eu.L^1]^+$. This difference in g_{em} values is readily explained in terms of the differing binding modes. Thus, the selective ligation of the carboxylate moiety in $[Eu.L^2]^+$ places the chiral centre (determining the relative disposition of the OH and Me groups) further away from the chiral element defining the metal helicity (i.e., in this case, the two Eu-$NCCN_{py}$ torsion angles; see scheme 3).

4. Conclusions

The design and validation of a modular CPL spectrometer is reported. Using two different Ln^{III} complexes, protein and anion binding can be sensitively monitored by observing a strong CPL signal. The helicity of the lanthanide complex is determined by the configuration of the added anion or protein.

In the binding of lactate to the lanthanide centre, when lactate is able to form a five-ring chelate, the g_{em} values are an order of magnitude greater than when the carboxylate oxygens bind cooperatively. Such behaviour accords with the increased distance between the lactate stereogenic centre in the latter case. Thus, there is a lesser steric preference for the relative positioning of the substituents around the chiral centre, which, in turn, induces the preferred metal complex helicity.

Samples of lactate exhibit a linear dependence of the emission dissymmetry factor with enantiomeric purity, suggesting that CPL can be used to assess enantiomeric purity in samples of unknown enantiomeric composition. The potential of monitoring an induced CPL to track changes in the local chiral environment of the lanthanide probe complex is therefore demonstrated.

Acknowledgments

We thank EPSRC and the ERC (DP, BKM, RP: *FCC 266804*), The Royal Society (LOP) for support and Mr Alexander G Wadham for contributions to instrument development. Dr Robert D Peacock is acknowledged for the preliminary measurements of data in figure 5.

References

[1] Riehl J P and Muller G 2012 *Comprehensive Chiroptical Spectroscopy: Instrumentation, Methodologies and Theoretical Simulations* (Hoboken, NJ: Wiley)

[2] Carr R, Evans N H and Parker D 2012 Lanthanide complexes as chiral probes exploiting circularly polarized luminescence *Chem. Soc. Rev.* **41** 7673

[3] Moore E G, Samuel A P S and Raymond K N 2009 From antenna to assay—lessons learned in lanthanide luminescence *Acc. Chem. Res.* **42** 542

[4] Riehl J P and Richardson F S 1986 Circularly polarized luminescence spectroscopy *Chem. Rev.* **86** 1

[5] Muller G 2009 Luminescent chiral lanthanide(III) complexes as potential molecular probes *Dalton Trans.* 9692

[6] Butler S J and Parker D 2013 Anion binding in water at lanthanide centres *Chem. Soc. Rev.* **42** 1652

[7] Trinquet E *et al* 2006 D-myo-inositol 1-phosphate as a surrogate of D-myo-inositol 1,4,5-tris phosphate to monitor G protein-coupled receptor activation *Anal. Biochem.* **358** 126

[8] Qang Q, Nono K N, Syrjanpaa N, Charbonniere L, Hovinen J and Harma H 2013 Stable and highly fluorescent europium chelates for time-resolved immunoassays *Inorg. Chem.* **52** 8461

[9] Lima L M P and Tripier R 2011 Cyclen-based lanthanide complexes as luminescent anion receptors *Curr. Methods Inorg. Chem.* **1** 36

[10] Schaferling M and Wolfbeis O S 2007 Europium tetracycline as luminescent probe for nucleoside phosphates, and its application for the determination of kinase activity *Chem.—Eur. J.* **13** 4342

[11] Lunkley J L, Shirotani D, Yamanari K, Kaizaki S and Muller G 2011 Chiroptical spectra of a series of tetrakis((+)-3-heptafluorobutylyrylcamphorato) lanthanide(III) with an encapsulated alkali metal ion: circularly polarized luminescence and absolute chiral structures for the Eu(III) and Sm(III) complexes *Inorg. Chem.* **50** 12724

[12] Dickins R S, Parker D, Bruce J I and Tozer D 2003 Correlation of optical and NMR spectral information with coordination variation for axially symmetric macrocyclic Eu(III) and Yb(III) complexes: axial donor polarisability determines ligand field and cation donor preference *Dalton Trans.* 1264

[13] Bruce J I *et al* 2000 The selectivity of reversible oxy-anion binding in aqueous solution at a europium and terbium centre; signalling of carbonate chelation by changes in the form and circular polarisation of luminescence emission *J. Am. Chem. Soc.* **122** 9674

[14] Pal R and Parker D 2009 An europium luminescence assay of lactate and citrate in biological fluids *Org. Biomol. Chem.* **7** 1525

[15] Poole R, Kielar F, Richardson S L, Stenson P A and Parker D 2006 A ratiometric and non-enzymatic luminescence assay for uric acid: differential quenching of lanthanide excited states by anti-oxidants *Chem. Commun.* 4084

[16] dos Santos C M G, Harte A J and Gunnlaugsson T 2008 Recent developments in the field of supramolecular lanthanide luminescent sensors and self-assemblies *Coord. Chem. Rev.* **252** 2512

[17] Carr R, Di Bari L, Lo Pino S, Parker D, Peacock R D and Sanderson J M 2012 A chiral probe for the acute phase proteins alpha-1-acid glycoprotein and alpha-1-antitrypsin based on europium luminescence *Dalton Trans.* **41** 13154

[18] Butler S J, Pal R, Pal R, Parker D and Walton J W 2013 Bright mono-aqua europium complexes based on triazacyclononane that bind anions reversibly and permeate cells efficiently *Chem. Eur. J.* **19** 9511

[19] Dickins R S *et al* 2002 Structural, luminescence and NMR studies of the reversible binding of acetate, lactate, citrate and selected amino-acids to chiral di-aqua ytterbium and europium complexes *J. Am. Chem. Soc.* **124** 12697

[20] Dickins R S, Batsanov A S, Parker D, Puschmann H, Salamano S and Howard J A K 2004 Structural and NMR investigations of the ternary adducts of twenty alpha amino-acids and selected dipeptides with a chiral, diaqua-ytterbium complex *Dalton Trans.* 70

[21] Cable M L, Kirby J P, Sorasaenee K, Gray H B and Ponce A 2010 Bacterial spore detection by [Tb^{3+}(macrocycle)(dipicolinate)] luminescence *J. Am. Chem. Soc.* **129** 1474

[22] Beeby A, Clarkson I M, Dickins R S, Faulkner S, Parker D, Royle L, de Sousa A, Williams J A G and Woods M 1999 Non-radiative deactivation of the excited states of europium, terbium and ytterbium complexes by proximate energy-matched OH, NH and CH oscillators: an improved luminescence method for establishing solution hydration states *J. Chem. Soc. Perkin Trans. 2* 493

[23] Walton J W, Di Bari L, Parker D, Pescitelli G, Puschmann H and Yufit D S 2011 Structure, resolution and chiroptical analysis of stable lanthanide complexes of a pyridylphenylphosphinate triazacyclononane ligand *Chem. Commun.* **47** 12289

[24] Walton J W, Carr R, Evans N H, Funk A M, Kenwright A M, Parker D, Yufit D S, Botta M, de Pinto S and Wong K-L 2012 Isostructural series of chiral nine-coordinate lanthanide complexes based on triazacyclononane *Inorg. Chem.* **51** 8042

[25] Evans N H, Carr R, Delbianco M, Pal R, Yufit D S and Parker D 2013 Complete stereocontrol in formation of macrocyclic lanthanide complexes: direct formation of enantiopure systems for circularly polarised luminescence applications *Dalton Trans.* **42** 15610